NRC Publications Archive
Archives des publications du CNRC

Electrocatalytic activity of non-stoichiometric perovskites toward oxygen reduction reaction in alkaline electrolytes

Yuan, Xiao-Zi; Li, Xiaoxia; Qu, Wei; Ivey, Douglas G.; Wang, Haijiang

NRC Publications Record / Notice d'Archives des publications de CNRC:
https://nrc-publications.canada.ca/eng/view/object/?id=4b829105-b537-4326-a288-9ef00537639f
https://publications-cnrc.canada.ca/fra/voir/objet/?id=4b829105-b537-4326-a288-9ef00537639f

Questions? Contact the NRC Publications Archive team at
PublicationsArchive-ArchivesPublications@nrc-cnrc.gc.ca. If you wish to email the authors directly, please see the first page of the publication for their contact information.

Vous avez des questions? Nous pouvons vous aider. Pour communiquer directement avec un auteur, consultez la première page de la revue dans laquelle son article a été publié afin de trouver ses coordonnées. Si vous n'arrivez pas à les repérer, communiquez avec nous à PublicationsArchive-ArchivesPublications@nrc-cnrc.gc.ca.

National Research Council Canada   Conseil national de recherches Canada

Canada

Electrocatalytic Activity of Non-Stoichiometric Perovskites toward Oxygen Reduction Reaction in Alkaline Electrolytes

Xiao-Zi Yuan[a], Xiaoxia Li[a], Wei Qu[a,*], Douglas G. Ivey[b], Haijiang Wang[a]

[a] National Research Council, Institute for Fuel Cell Innovation
Vancouver, BC, Canada, V6P 1W5
[b] Department of Chemical and Materials Engineering
University of Alberta, Edmonton, AB, Canada T6G 2V4

Perovskite $La_xCa_{0.4}MnO_3$ (x = 0.4, 0.5, 0.6) powder was prepared through a sol-gel method and characterized by X-ray diffraction (XRD), a gas adsorption technique (BET) and transmission electron microscopy (TEM). The electrocatalytic properties of $La_xCa_{0.4}MnO_3$/C composites towards the oxygen reduction reaction (ORR) were studied using rotating ring-disk electrode (RRDE) techniques and Koutecky-Levich theory in both 1 M and 6 M KOH electrolytes. The results show better ORR activities for non-stoichiometric perovskites than that for stoichiometric $La_{0.6}Ca_{0.4}MnO_3$. The overall electron transfer numbers for these $La_xCa_{0.4}MnO_3$ composites are in the range of 3.2-3.7, and with decreasing values of x the electron transfer number increases and accordingly H_2O_2 production decreases. These results suggest that the existence of a Mn reduction/oxidation pair in Ca-doped nonstoichiometric perovskites could activate the ORR reaction sites, resulting in improved catalytic activity.

Introduction

One advantage of developing alkaline-based fuel cells and metal air batteries is the possibility of using low cost, non-noble catalysts for the oxygen reduction reaction (ORR) [1][2]. The lanthanum-based, perovskite-type oxides ($LnBO_3$, Ln= La or partially substituted by Ca or Sr; B= Co, Mn or Fe) are promising candidates for air-electrodes or even bifunctional air-electrodes due to their sufficient activities towards oxygen reduction and oxygen evolution reactions, as well as good electrochemical stability in concentrated alkaline electrolytes [3][4]. Yamazoe et al. [5] analyzed the ORR mechanisms catalyzed by perovskites using both iodometry and electron spin resonance, and suggested that ORR could proceed favorably at the active sites of Mn^{3+}/Mn^{4+} pairs on perovskite surfaces. The Mn^{3+}/Mn^{4+} pair can be formed by partial substitution of La^{3+} with Na^+, K^+ or Rb^+. Mn^{4+} may drive electron exchange within the perovskite structure by capturing an electron from neighboring Mn^{3+} [6] and then activate the reaction sites for ORR. In this study, we have designed and synthesized Ca-doped non-stoichiometric perovskites $La_xCa_{0.4}MnO_3$ (x= 0.4, 0.5, 0.6) in an attempt to activate the ORR reaction sites with Mn

* Corresponding author. Email: Wei.Qu@nrc-cnrc.gc.ca, Tel: 1-604-221-3061, Fax: 1-604-221-3001

ions in the perovskite lattice. The ORR activities of Ca-doped non-stoichiometric and stoichiometric $La_xCa_{0.4}MnO_3$, in both 1M and 6 M KOH electrolytes, are compared.

Experimental

Synthesis and structure characterization

$La_xCa_{0.4}MnO_3$ powder was prepared using citric acid, lanthanum nitrate, calcium nitrate and manganese nitrate to form the precursor, followed by heat treatment in an air atmosphere at 650^oC for 5 hours. The crystal phase of the $La_xCa_{0.4}MnO_3$ powder was assessed by X-ray diffraction (XRD) with a Bruker D8 advanced diffractometer (Cu K-α1 source, λ= 1.5406 Å) over the range of 10-90º at a scanning rate of $0.1º\ s^{-1}$. Specific surface area measurements were carried out using the Brunauer Emmett Teller (BET) gas adsorption technique on a surface area analyzer (SA3100, Beckman Coulter). The morphology and particle size were observed by transmission electron microscopy (TEM) using an FEI Tecnai G2 TEM/STEM.

Working electrode preparation

The electrochemical properties of $La_xCa_{0.4}MnO_3$ were evaluated using a $La_xCa_{0.4}MnO_3$ composite ($La_xCa_{0.4}MnO_3/C$) with the catalyst supported on Vulcan 72 carbon (BET surface area of 222 m^2g^{-1}). The $La_xCa_{0.4}MnO_3/C$ electrode layer was prepared on a glassy carbon (GC) disk of the rotating-ring disk electrode (RRDE) tip (AFE7R9GCPT, Pine Research Inc.) by coating a layer of ultrasonically mixed $La_xCa_{0.4}MnO_3$ and C powder ink with a composite loading of 250 $ugcm^{-2}$. On top of this electrode layer a 4.0 μL, 0.5 wt% Nafion® solution was then pipetted, followed by a drying process using a 20 W lamp.

Electrochemical measurements

A conventional three-electrode electrochemical cell was used for all cyclic voltammetry (CV) and RRDE measurements, which were conducted on a Solartron Analytical 1470E system, as described elsewhere [7]-[9]. The ring electrode collection efficiency of this RRDE was measured to be 0.20±0.01. Before taking cyclic voltammetry measurements, the solution was bubbled with pure N_2 (99.99%) for at least 30 minutes to remove any dissolved O_2. For ORR measurements, the solution was saturated by bubbling pure O_2 (99.99%) for at least 30 minutes.

Results and Discussions

Structure and morphology characterization

Figure 1 shows high-resolution XRD patterns of the synthesized materials. It can be seen that the XRD patterns are almost identical to the standard patterns (JCPDS File #00-046-0513), which can be readily indexed to the orthorhombic phase of $La_{0.6}Ca_{0.4}CoO_3$ (space group: Pnma). There were no additional peaks detected for either La_2O_3 or CoO_x. However, two small peaks, marked with asterisks in the spectrum, were observed but have not been identified. BET measurements were also conducted for these materials, giving a surface area of ~30 m^2g^{-1} for all the samples.
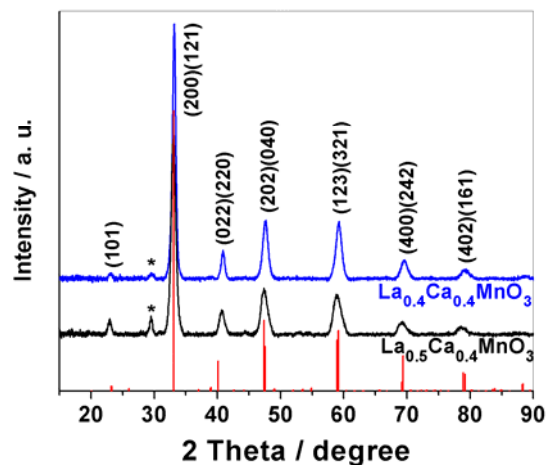
Figure 1. Typical XRD patterns for the La$_x$Ca$_{0.4}$MnO$_3$ perovskites. The standard pattern for La$_{0.6}$Ca$_{0.4}$CoO$_3$ is shown as vertical lines.
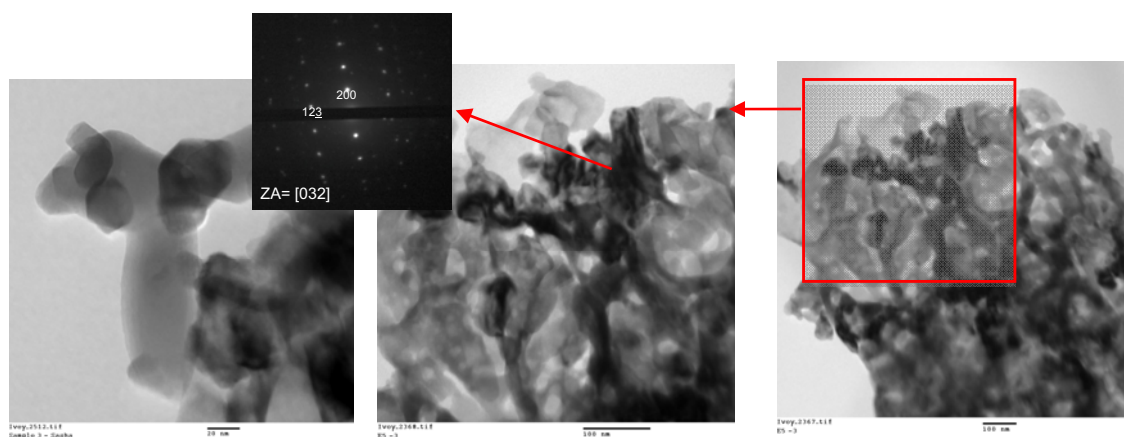

Figure 2. TEM bright field (BF) images and electron diffraction pattern for the La$_{0.4}$Ca$_{0.4}$MnO$_3$ sample.

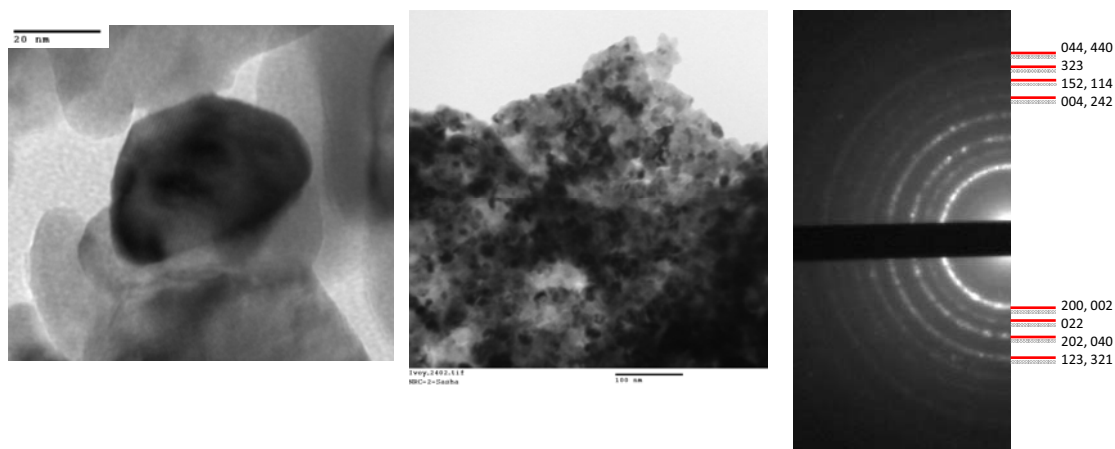Figure 3. TEM BF images and electron diffraction pattern for the La$_{0.5}$Ca$_{0.4}$MnO$_3$ sample. The diffraction pattern is from the entire field of view.

Figures 2 to 4 show TEM images and electron diffraction patterns for samples $La_{0.4}Ca_{0.4}MnO_3$, $La_{0.5}Ca_{0.4}MnO_3$, and $La_{0.6}Ca_{0.4}MnO_3$, respectively. From the electron diffraction patterns, the crystal structures of $La_{0.4}Ca_{0.4}MnO_3$, $La_{0.5}Ca_{0.4}MnO_3$, and $La_{0.6}Ca_{0.4}MnO_3$ can all be indexed to orthorhombic $La_{0.6}Ca_{0.4}MnO_3$ (00-046-0513) with a= 0.5443 nm, b= 0.7683 nm, and c= 0.5454 nm, which agrees with the XRD results. The particle sizes for all samples are in the range of 20-30 nm.
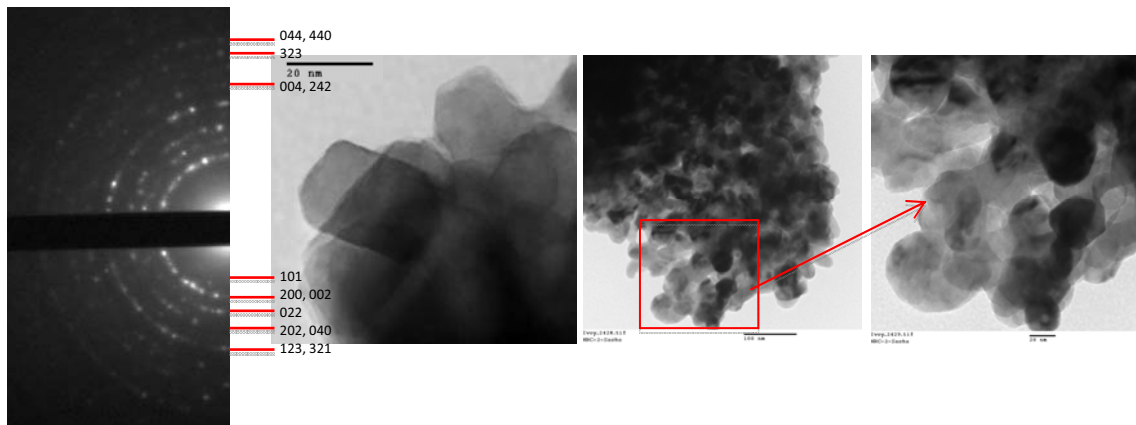

Figure 4. TEM BF images and electron diffraction pattern for the $La_{0.6}Ca_{0.4}MnO_3$ sample. The diffraction pattern is from the entire field of view.

Electrocatalytic activities towards ORR

The cyclic voltammetric (CV) characteristics of the synthesized $La_xCa_{0.4}MnO_3$ material are compared over the potential range of –0.70 to +0.30 V vs. Hg/HgO in N_2- and O_2-saturated 1 M and 6 M KOH solutions. Figure 5 shows typical CV curves using $La_{0.6}Ca_{0.4}MnO_3$ as an example. Similar curves were obtained for $La_{0.4}Ca_{0.4}MnO_3$ and $La_{0.5}Ca_{0.4}MnO_3$ as well. As seen in Figure 5, in the negative sweep to low potentials, a downward peak is observed at –0.07 V, which can be ascribed to the ORR. Another downward broad peak at -0.37 V is related to Mn ion reduction, which is oxidized at about 0.06 V in the positive sweep to high potentials.
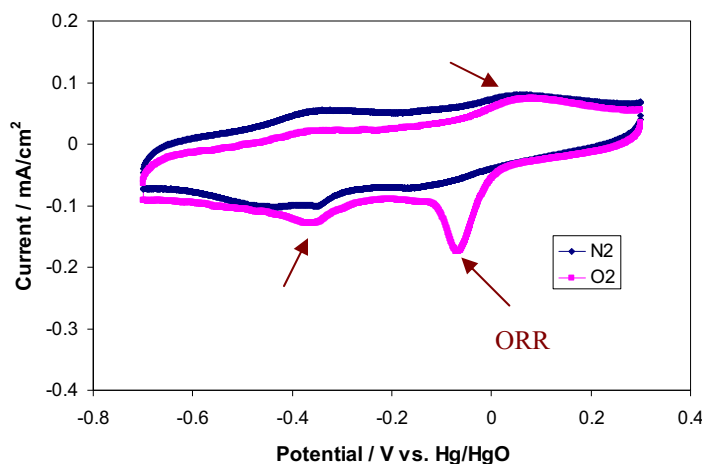

Figure 5. Comparison of CV curves for $La_{0.6}Ca_{0.4}MnO_3$ perovskite electrode in N_2 and O_2 environments (5 mV/s, 6 M KOH).

To verify the existence of the Mn oxidation and reduction pair, an extra experiment was designed, and the result is plotted in Figure 6. As shown in Figure 6, Mn reduction and oxidation occur at about -0.32 V and 0.08 V vs. Hg/HgO, which match the peaks in Figure 5. The small potential differences may be due to the electrolyte concentration and the catalyst type. For example, the ORR occurs in Figure 6 at about -0.10V, which is a shift of about 30 mV from –0.07 V in Figure 5. These results confirm the existence of a Mn reduction/oxidation pair, Mn^{3+}/Mn^{4+} being the possible pair [1]. The observed ORR activities suggest that $La_xCa_{0.4}MnO_3$ materials synthesized in this work could be a candidate for the air cathode.
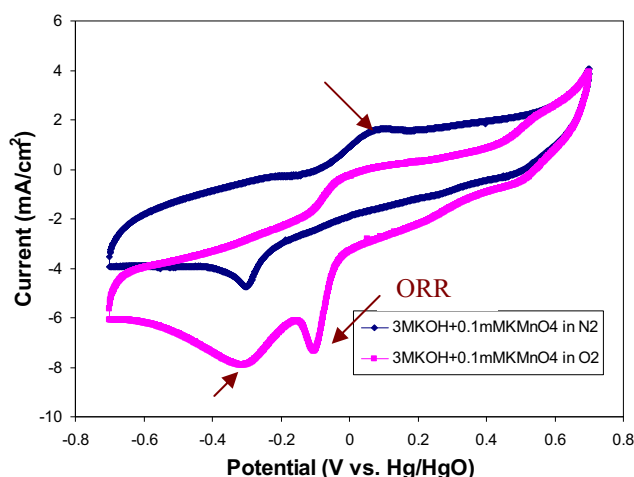

Figure 6. Comparison of Mn activity in the presence of $KMnO_4$ in N_2 and O_2 (commercial CoTMPP electrode, 25 mV/s, 3 M KOH).
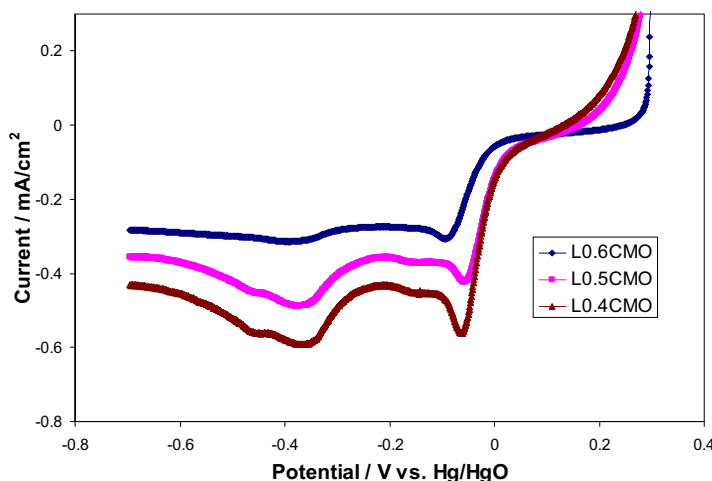

Figure 7. ORR curves for $La_xCa_{0.4}MnO_3$/C perovskite electrodes over the potential range of –0.70 to +0.30 V vs. Hg/HgO (1600 rpm, 5 mV/s, 6 M KOH).

ORR activities of the electrode coated with these three materials are compared in Figure 7. The ORR activity of non-stoichiometric Ca-doped perovskites, $La_{0.4}Ca_{0.4}MnO_3$ ($L_{0.4}CMO$) and $La_{0.5}Ca_{0.4}MnO_3$ ($L_{0.5}CMO$), is better than that of stoichiometric $La_{0.6}Ca_{0.4}MnO_3$ ($L_{0.6}CMO$) with a higher Mn reduction peak, suggesting that the formation of the Mn reduction/oxidation pair in Ca-doped nonstoichiometric perovskites could activate the ORR reaction sites, resulting in improved catalytic activity.

ORR kinetics

For more quantitative evaluation of the ORR activities of $La_xCa_{0.4}MnO_3$-based electrodes, the RRDE technique was employed to obtain the overall electron transfer number by applying the Koutecky-Levich theory. Figures 8-10 show the disk and ring currents collected on rotated $La_{0.4}Ca_{0.4}MnO_3/C$, $La_{0.5}Ca_{0.4}MnO_3/C$ and $La_{0.6}Ca_{0.4}MnO_3/C$ electrodes, respectively, at different rates from 900 to 2500 rpm in O_2-saturated 1 M and 6 M KOH electrolytes.

Figure 8. RRDE curves for the $La_{0.4}Ca_{0.4}MnO_3$ electrode in an O_2-saturated environment. The ring potential was fixed at 0.5 V (vs. Hg/HgO) with a scan rate of 5 mV/s.

Figure 9. RRDE curves for the $La_{0.5}Ca_{0.4}MnO_3$ electrode in an O_2-saturated environment. The ring potential was fixed at 0.5 V (vs. Hg/HgO) with a scan rate of 5 mV/s.
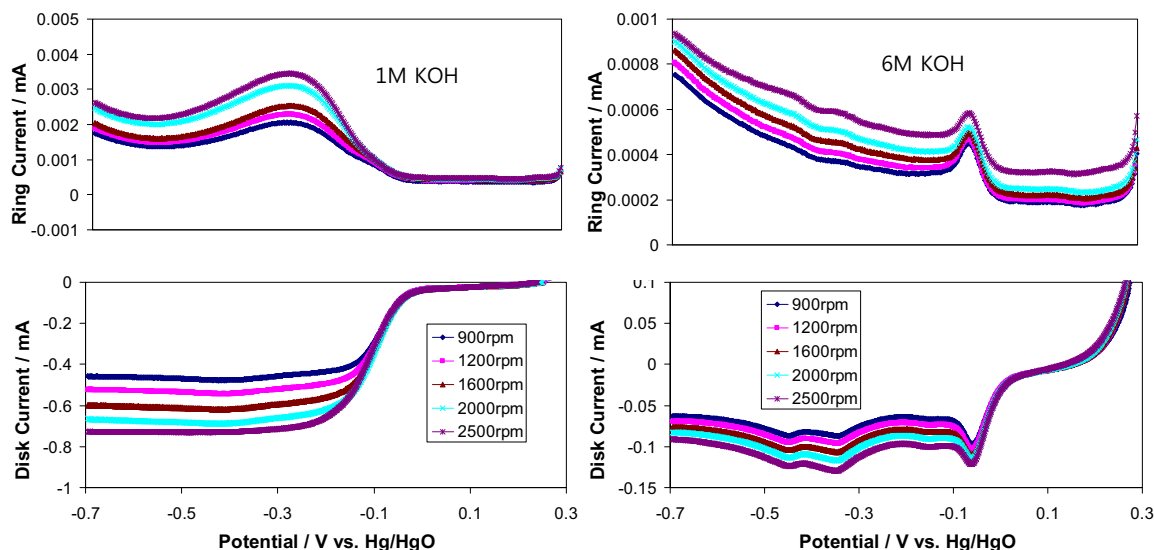
Figure 10. RRDE curves for the $La_{0.6}Ca_{0.4}MnO_3$ electrode in an O_2-saturated environment. The ring potential was fixed at 0.5 V (vs. Hg/HgO) with a scan rate of 5mV/s.

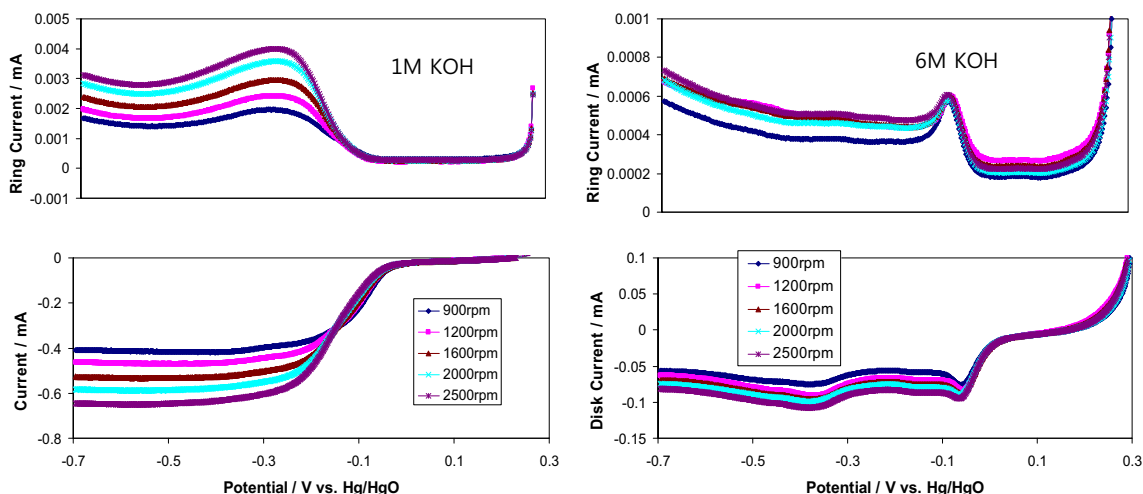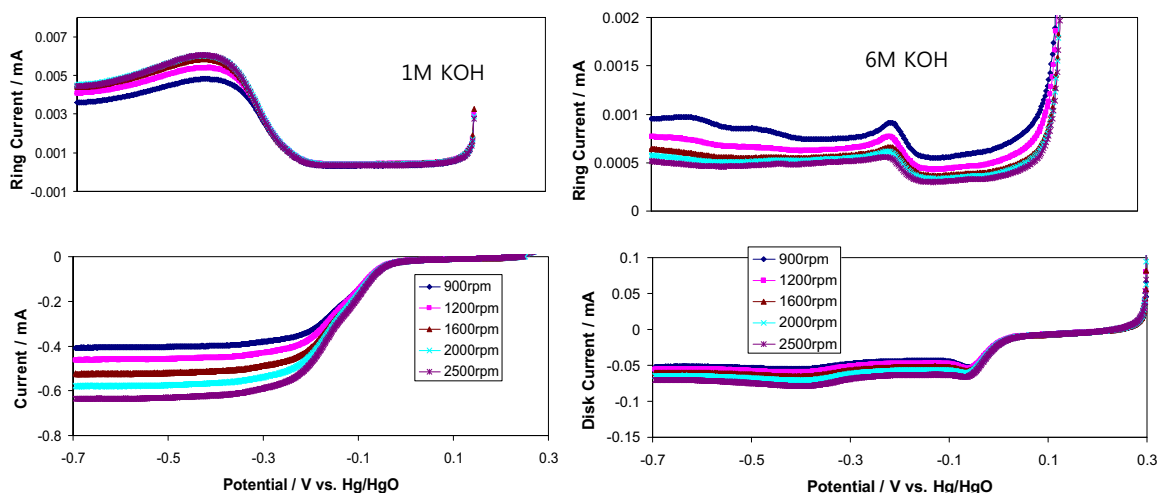Compared to samples in the 1 M KOH electrolyte, the diffusion current in 6 M KOH is about 10 times smaller due to the decreased solubility and diffusion coefficient of oxygen, as well as the increased kinematic viscosity of the electrolyte at a higher KOH concentration, which agrees with our previous results [8]. According to Koutecky-Levich theory [10]:

$$i_{dl} = 0.201nFAC_{O_2}D_{O_2}^{2/3}\nu^{-1/6}\omega^{1/2} = Bn\omega^{1/2} \qquad [1]$$

where i_{dl} is the diffusion-limiting current, n is the overall electron transfer number in ORR, F is the Faraday constant (96500 C mol^{-1}), A is the geometric area of the disk electrode (0.16 cm^2), C_{O_2} (mol cm^{-3}) is the oxygen concentration dissolved in the electrolyte solution, D_{O_2} (cm^2 s^{-1}) is the diffusion coefficient of oxygen, ν (cm^2 s^{-1}) is the kinematic viscosity of the electrolyte and ω (rpm) is the electrode rotation rate.

From Figures 8-10, the Koutecky-Levich (K-L) plots can be plotted for the $La_xCa_{0.4}MnO_3$/C electrodes in two KOH concentrations, as shown in Figure 11. These theoretical plots were calculated based on the parameters reported in the literature [11][12] and are listed in Table 1. Activity coefficients for 1 M and 6 M KOH are also included. The K-L plots show linear and parallel features in both 1 M and 6 M KOH for all the electrodes, confirming first-order kinetics with respect to oxygen concentration [13]. The slopes of the K-L plots were calculated to be close to the values of theoretical 4-electron transfer on all electrodes, suggesting that the ORR process catalyzed by $La_xCa_{0.4}MnO_3$ is dominated by a 4-electron transfer pathway. The overall electron transfer numbers calculated from the slope range from 3.2-3.7 in all the three cases and the number decreases with increasing values of x. This result suggests that the ORR activity of non-stoichiometric $La_xCa_{0.4}MnO_3$ is better than that of stoichiometric $La_xCa_{0.4}MnO_3$, which further confirms that the formation of a Mn reduction/oxidation pair in Ca-doped nonstoichiometric perovskites can activate the ORR reaction sites, resulting in improved catalytic activity.
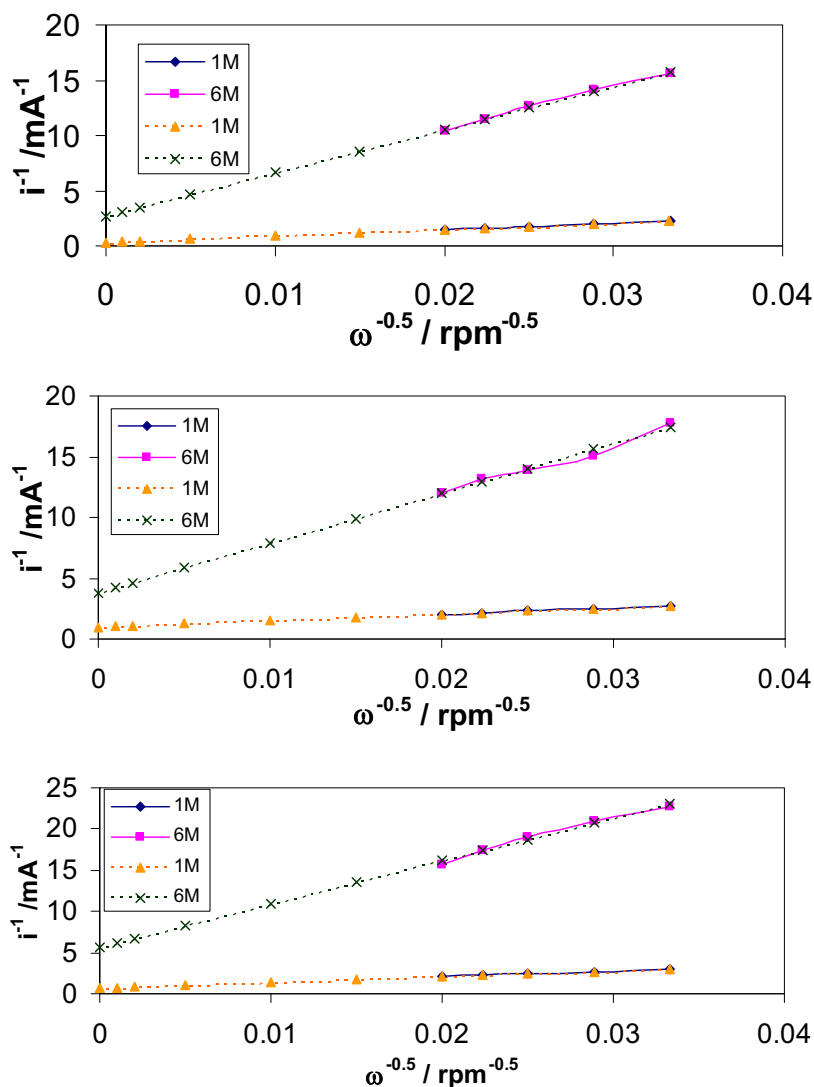
Figure 11. ORR Koutecky-Levich plots for (a) $La_{0.4}Ca_{0.4}MnO_3$, (b) $La_{0.5}Ca_{0.4}MnO_3$ and (c) $La_{0.6}Ca_{0.4}MnO_3$ electrodes in O_2-saturated KOH solutions.

Table 1 Parameters used for calculating overall electron transfer numbers

Electrolyte solutions	C_{O_2} mol cm^{-3}	D_{O_2} cm^2 s^{-1}	v cm^2 s^{-1}	Density g cm^{-3}	Activity coefficient
1 M	0.83×10^{-6}	1.65×10^{-5}	0.95×10^{-2}	1.045	0.731
6 M	0.17×10^{-6}	0.78×10^{-5}	1.52×10^{-2}	1.253	1.638

RRDE measurements

The overall electron number (n) of the ORR on the electrodes can also be calculated from the ratio of disk and ring currents in RRDE measurements. According to the RRDE theory, the overall electron transfer numbers and the corresponding mole

percentage of H_2O_2 produced (mol% H_2O_2) in the ORR process can be determined using Equations [2] and [3], respectively [14] [15]:

$$n = \frac{4i_d}{i_d + (i_r / N)} \qquad [2]$$

$$\%H_2O_2 = \frac{100(i_r / i_d)}{N} \qquad [3]$$

where i_d is the current on the disk electrode, i_r is the current on the ring electrode, and N is the collection coefficient of the ring electrode (0.20±0.01). The overall electron transfer numbers in the ORR process were calculated over a potential range from –0.20 V to –0.50 V at 1600 rpm in both 1 M and 6 M KOH, as presented in Figure 12. It can be seen that the electron transfer numbers for all the electrodes are in the range of 3.2-3.7 in both electrolytes, which corresponds to 8-24% of H_2O_2 production. The results are in good agreement to the results estimated from K-L plots in Figure 11.
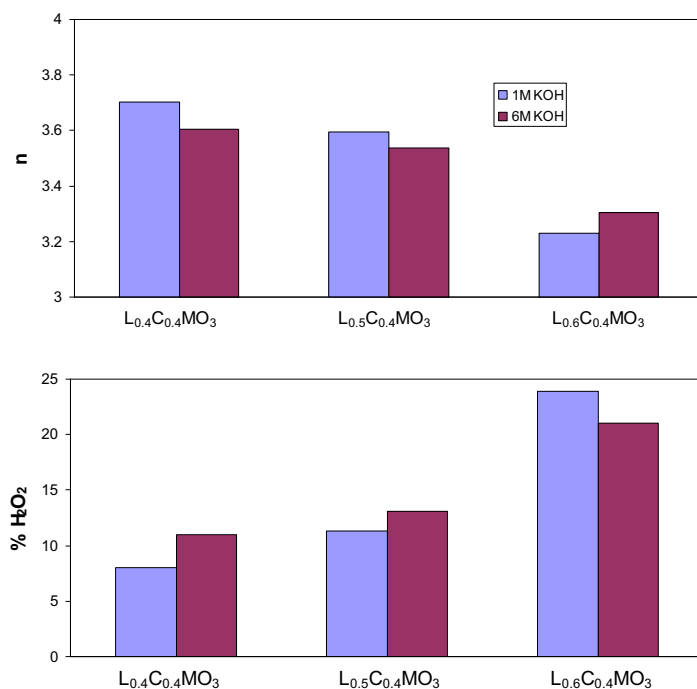

Figure 12. (a) ORR overall electron transfer numbers and (b) hydrogen peroxide production obtained using RRDE electrodes coated with $La_xCa_{0.4}MnO_3/C$ in O_2-saturated 1 M and 6 M KOH electrolytes. The electrode was rotated at 1600rpm. The experimental conditions were the same as displayed in Figures 8-10.

Conclusions

Perovskite $La_xCa_{0.4}CoO_3$ was successfully synthesized using a sol-gel method and characterized by XRD, BET and TEM. The BET measurements show that all the synthesized materials have a surface area of ~30 m^2g^{-1}. The XRD and TEM confirm that all non-stoichiometric $La_xCa_{0.4}MnO_3$ can be indexed to orthorhombic $La_{0.6}Ca_{0.4}MnO_3$ with a particle size ranging from 20-30 nm. The $La_xCa_{0.4}CoO_3$ materials were also

electrochemically characterized for ORR in both 1 M and 6 M KOH electrolytes. All electrodes show activity towards ORR, but non-stoichiometric $La_xCa_{0.4}MnO_3$ perovskites display better activity than stoichiometric $La_xCa_{0.4}MnO_3$, suggesting that the existence of a Mn reduction/oxidation pair in Ca-doped nonstoichiometric perovskites could activate the ORR reaction sites, resulting in improved catalytic activity. RRDE results exhibit that the electron transfer numbers on all the electrodes are in the range of 3.2-3.7 in both studied KOH concentrations, which corresponds to 8-24% of H_2O_2 production, indicating that the ORR process catalyzed by $La_xCa_{0.4}MnO_3$ is dominated by a 4-electron transfer pathway. Decreasing the value of x results in an increase in the electron transfer number, which further confirms the improved ORR activity of Ca-doped nonstoichiometric perovskites.

Acknowledgements

References

[1]   H. Arai, S. Müller, O. Haas, *J. Electrochem. Soc.*, **147 (10)**, 3584 (2000).

[2]   J. Goldstein, I. Brown, B. Koretz, *J. Power Sources*, **80**, 171 (1999).

[3]   J. Tulloch, and S. W. Donne, *J. Power Sources*, **188**, 359 (2009).

[4]   S.W. Eom, S. Y. Ahn, C.W. Lee, Y.K. Sun, M.S. Yun, *Solid State Phenomena*, **124-126**, 1055 (2007).

[5]   A. Hayashi, T. Hyodo, N. Miura, N. Yamazoe, *Electrochem.*, **6(2)**, 112 (2000).

[6]   C. Zener, *Phys. Rev.*, **82**, 403 (1951).

[7]   X.X. Li, W. Qu, H. Wang, R. Hui, L. Zhang, J. Zhang, *Electrochim. Acta,* **55**, 5891 (2010).

[8]   X.X. Li, W. Qu, J. Zhang, H. Wang, *ECS Trans.*, **28**, 45 (2010).

[9]   X.X. Li, W. Qu, J. Zhang, H. Wang, *J. Electrochem. Soc.*, **158**, A597 (2011).

[10] A.J. Bard, L.R. Faulkner, Electrochemical Methods: Fundamentals and Applications, 2nd ed., John Wiley & Sons, New York, 2001.

[11] K.E. Gubbins, R. D. Walker, *J. Electrochem. Soc.*, **112**, 469 (1965).

[12] D.R. Lide (ed.), CRC Handbook of Chemistry and Physics, CRC Press, 90th Edition, 2009-2010.

[13] H. Meng, P.K. Shen, *Electrochem. Comm.,* **8**, 588 (2006).

[14] C.B. Bezerra, L. Zhang, K.C. Lee, H.S. Liu, J.L. Zhang, Z. Shi, A.L.B. Marques, E.P. Marques, S.H. Wu, J. Zhang, *Electrochim. Acta*, **53**, 7703 (2008).

[15] U.A. Paulus, T.J. Schmidt, H.A. Gasteiger, R.J. Behm, *J. Electroanal. Chem.*, **495**, 134 (2001).